

# Periodicity of Thalamic Synchronized Oscillations: the Role of $\text{Ca}^{2+}$ -Mediated Upregulation of $I_h$

Anita Luthi and David A. McCormick\*

Section of Neurobiology  
Yale University School of Medicine  
New Haven, Connecticut 06510

## Summary

Thalamocortical networks can generate both normal and abnormal patterns of synchronized network activity, such as spindle waves and spike-and-wave seizures. These periods of synchronized discharge are often separated by a silent, refractory phase of between 5 and 20 s. *In vitro* investigations have demonstrated that this refractory period is due in large part to the persistent activation of the hyperpolarization-activated cation current  $I_h$  in thalamocortical cells. Here, we show that increases in  $[\text{Ca}^{2+}]_i$  due to rebound  $\text{Ca}^{2+}$  bursts result in persistent activation of  $I_h$ , resulting from a positive shift in the activation curve of this current. The dynamical upregulation and persistent activation of  $I_h$  is the critical determinant of the time course of the refractory period. These findings demonstrate that periodicity in neural network oscillations may be generated through an interaction between the electrophysiological properties and intracellular signaling pathways of the constituent neurons.

## Introduction

The thalamus is the main gateway for information flow from the periphery to the cerebral cortex. During the waking and attentive state, thalamic cells discharge in a manner that is dictated in large part by the pattern of synaptic potentials arriving from prethalamic structures such as the retina or from the cerebral cortex (reviewed by Jones, 1985; Steriade et al., 1993; Steriade et al., 1997). In contrast, during slow-wave sleep, anesthesia, or an epileptic seizure, thalamic neurons generate synchronized network oscillations, many of which display slow periodicities on the order of seconds to tens of seconds (reviewed by Andersen and Andersson, 1968; Steriade et al., 1993; McCormick and Bal, 1997; Steriade et al., 1997).

Spindle waves are sleep-related rhythmic oscillations that occur as spontaneous 7–14 Hz activity that waxes and wanes over a 1–3 s period and recurs approximately once every 5–20 s (Andersen and Andersson, 1968; Steriade and Deschênes, 1984; Steriade et al., 1993; Kim et al., 1995; Contreras et al., 1997). In an *in vitro* slice preparation of ferret dorsal lateral geniculate nucleus (LGNd) exhibiting spontaneous spindle wave activity, the generation of these oscillations resides in a reciprocal interaction between two mutually interconnected types of cells, the GABAergic neurons of the thalamic

reticular–perigeniculate nuclei (PGN) and the glutamatergic thalamocortical cells (von Krosigk et al., 1993; Bal et al., 1995a, 1995b; Kim et al., 1995).

The 5–20 s refractory period in between spindle waves is associated with a small, slowly decaying after-depolarization (ADP) in thalamocortical cells that is caused by activation of the hyperpolarization-activated cation current  $I_h$  during the oscillatory activity (Bal and McCormick, 1996). This ADP is sufficiently large to decrease the probability of thalamocortical neurons to respond with a  $\text{Ca}^{2+}$  burst following the arrival of IPSPs from the PGN, thus causing the network activity to fade and to display a refractoriness to further oscillations. Activation and subsequent deactivation of  $I_h$  in thalamocortical cells thus appears to be a key mechanism through which synchronized oscillations are terminated and prevented within defined intervals (Leresche et al., 1991; Soltesz et al., 1991; Bal and McCormick, 1996; Lee and McCormick, 1996).

What are the physiological components of spindle waves and paroxysmal oscillations that are essential for activity-dependent, endogenous activation of  $I_h$ ? Evidently, the arrival of IPSPs during these oscillations induces repetitive membrane hyperpolarization, thus leading to voltage-dependent gating of  $I_h$ . However, these IPSPs are short in duration and small in amplitude and thus, in view of the slow activation kinetics of  $I_h$ , lead to only a partial activation of this current (McCormick and Pape, 1990a; Pape, 1996). Moreover, the deactivation kinetics of  $I_h$  at resting membrane potential are too fast to account for the prolonged, persistent ADP during the refractory period (Huguenard and McCormick, 1992; McCormick and Huguenard, 1992; Destexhe et al., 1996). One possibility is that biophysical properties of  $I_h$  are modulated as a result of preceding activity. Previous studies in cardiac cells have suggested that the pacemaking hyperpolarization-activated f-current, which is equivalent to the h-current, may be shifted in voltage dependence by increases in the intracellular concentration of free  $\text{Ca}^{2+}$  (Hagiwara and Irisawa, 1989). Computational models of synchronized thalamocortical activity indicate that shifts in the activation curve of  $I_h$  from activity-dependent increases in the concentration of an intracellular second messenger, such as  $\text{Ca}^{2+}$ , could account for the generation of the refractory period and the rhythmicity of synchronized oscillations (Destexhe et al., 1996).

In the present study, we demonstrate that the voltage dependence and kinetics of the hyperpolarization-activated cation current  $I_h$  are sensitive to the intracellular concentration of  $\text{Ca}^{2+}$ . We hypothesize that the  $\text{Ca}^{2+}$ -dependent upregulation of  $I_h$  is mediated through additional second messenger systems and is critical to the generation of slow, periodic rhythms in thalamocortical systems.

## Results

To characterize the activity-dependent activation of  $I_h$ , impaled thalamocortical neurons were injected with repetitive hyperpolarizing current pulses (2–8 Hz; Figure

\*To whom correspondence should be addressed.

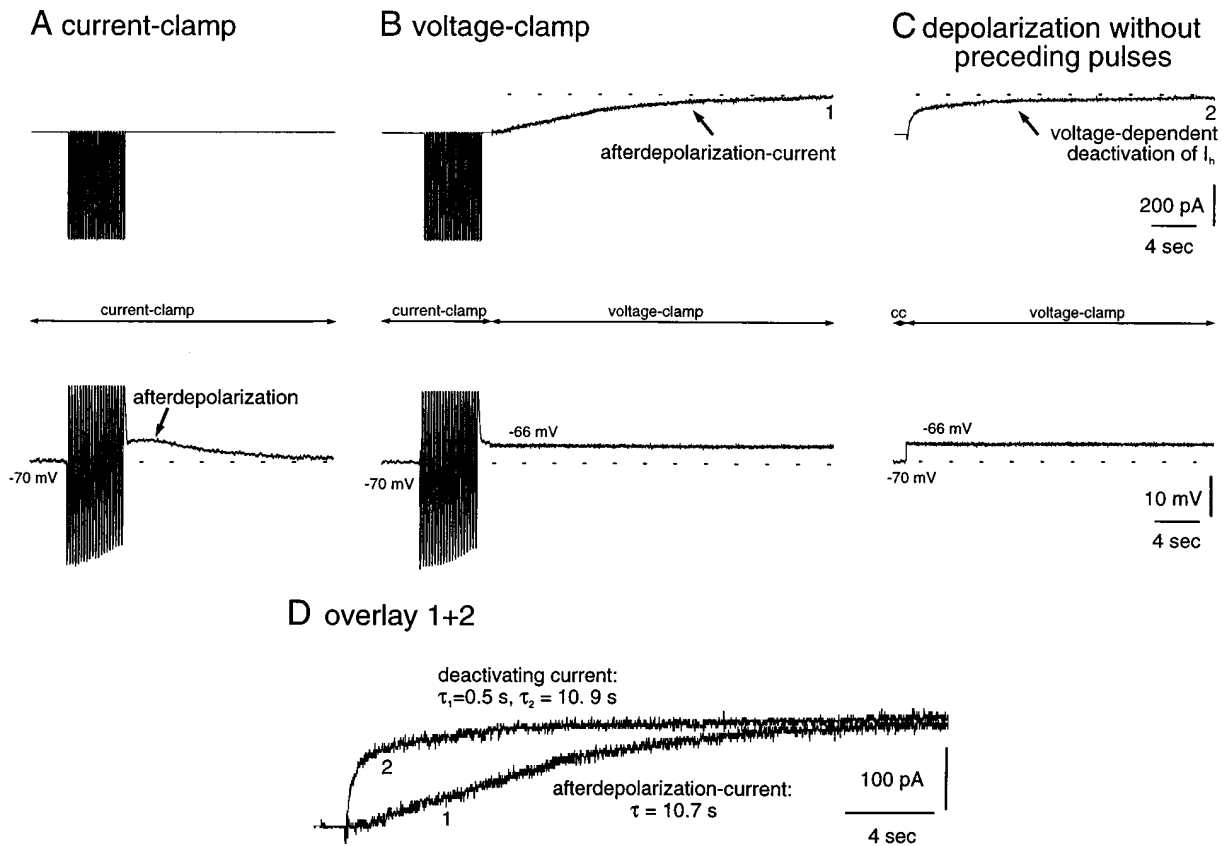


Figure 1. Repetitive Constant Current Injections into Thalamocortical Cells Mimicking the Generation of a Synchronized Oscillation Are Followed by an ADP Due to Persistent Activation of  $I_h$

(A) Repetitive constant current injections (4 Hz, 20 pulses, 120 ms; upper trace) generate a slowly decaying ADP (lower trace).  
 (B) Single-electrode voltage clamp of the cell at the peak potential of the ADP reveals a slowly decaying inward current, reflecting the decay of  $I_h$  responsible for the generation of the ADP.  
 (C) Voltage clamp of the cell at the peak potential of the ADP but without preceding hyperpolarizing current pulses reveals the decay kinetics of  $I_h$  due to voltage-dependent deactivation of this current.  
 (D) Overlay of the current responses from (B) and (C). Note the promotion of the slowly decaying form of  $I_h$  recorded following a train of repetitive current injections.

1A), evoking rebound  $Ca^{2+}$  bursts following each current pulse and mimicking the arrival of inhibitory inputs during synchronized network activity. Such patterns of current injections have been shown to produce an ADP that is indistinguishable in its characteristics and functional consequences on neuronal responses from the ADP induced during spontaneous network oscillations (Bal and McCormick, 1996). The advantage of studying the ADP generated by current injections rather than the ADP generated by spontaneous spindle waves is that the frequency, amplitude, and duration of hyperpolarizing current pulses and the number of rebound  $Ca^{2+}$  spikes can be accurately controlled, whereas the IPSPs arriving during spindle waves and their efficiency in evoking  $Ca^{2+}$  spikes vary from one wave to the next.

Activation of  $I_h$  was monitored in hybrid current/voltage-clamp experiments, in which repetitive hyperpolarizing pulses were delivered in the current-clamp mode and the membrane current during the time period of the ADP (ADP-current) was examined under single-electrode, voltage-clamp conditions by clamping the cell to the voltage corresponding to the peak of the ADP (Figure 1B). The ADP current was compared to that reflecting

the purely voltage-dependent deactivation of  $I_h$  (along with the activation and deactivation of other currents) obtained by clamping to the peak potential of the ADP but without preceding repetitive current injections (Figures 1C and 1D). At this voltage, the current developing following repetitive hyperpolarizing current pulses appeared as a slowly decaying inward current that was well fit with a single exponential function ( $\tau = 8.5 \pm 0.76$  s,  $n = 8$ ). In contrast, stepping to this membrane potential without the injection of the preceding hyperpolarizing current pulses resulted in an inward current that decayed biexponentially with a fast ( $\tau = 0.36 \pm 0.05$  s,  $n = 8$ ), followed by a small (32%  $\pm$  2.7% of total current,  $n = 8$ ), slowly decaying component ( $\tau = 7.14 \pm 0.8$  s,  $n = 7$ ; Figures 1C and 1D). Local application of the specific blockers of  $I_h$ ,  $Cs^+$  (20 mM in micropipette,  $n = 5$ ) and ZD7288 (1 mM,  $n = 6$ ; BoSmith et al., 1993; Harris and Constanti, 1995; Williams et al., 1997), abolished the ADP and the ADP-current (see also Bal and McCormick, 1996). One possible explanation of these findings is that repetitive current pulses induce an alteration of the biophysical properties of  $I_h$ , favoring the persistent activation of  $I_h$  and a correspondingly slower

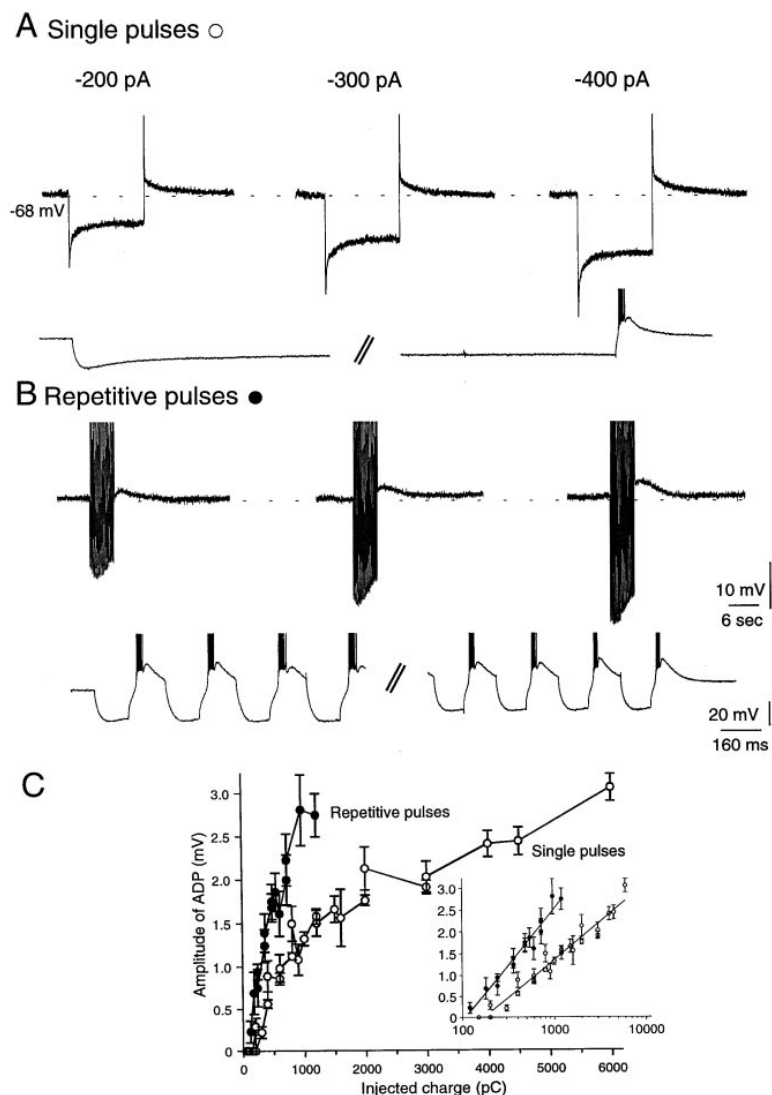


Figure 2. Repetitive Constant Current Pulses that Evoke Rebound Ca<sup>2+</sup> Spikes Are More Efficient in Generating an ADP Than Are Single, Long-Duration Current Injections that Generate Only One Rebound Ca<sup>2+</sup> Spike

(A) ADPs recorded following injections of one hyperpolarizing current pulse, the amplitude of which is indicated above the recorded traces. The trace below denotes the membrane potential trajectory of one response at an expanded time scale. Each current injection hyperpolarizes the cell and induces a depolarizing deviation of the membrane potential, followed by a single rebound Ca<sup>2+</sup> spike at the offset of the pulse.

(B) ADPs recorded following injections of 20 repetitive hyperpolarizing current pulses. The trace below denotes the membrane potential trajectory of one response at an expanded time scale. Each current pulse is followed by a rebound Ca<sup>2+</sup> spike.

(C) Plots of the amplitude of the ADP as a function of the total hyperpolarizing charge injected (for single pulses, time of pulse × amplitude of current injection; for repetitive pulses, time of each single pulse × number of pulses) demonstrate that with the same amount of total charge injected, a larger ADP is generated with repetitive pulses (closed circles) than with a single pulse (open circles). The inset plots the same data on a semi-logarithmic scale. Data have been fitted by linear regression to the function:  $a \times \log_{10}x + b$ ;  $a$  and  $b$  are 2.6 mV and  $-5.3$  mV for repetitive pulses and 1.75 mV and  $-3.9$  mV for single pulses, respectively. Thus, for a 10-fold increase in injected charge, the ADP increases by 2.6 mV with repetitive and only by 1.75 mV with single pulses. Correlation coefficient for both fits,  $r = 0.98$ . Data in (A) and (B) are from the same cell. Scale bars depicted in (B) hold for the corresponding traces in (A).

decay of this current. The induction of a persistent activation of I<sub>h</sub>, obtained here following application of a series of hyperpolarizing current injections mimicking inhibitory input during synchronized oscillations, is referred to as “upregulation of I<sub>h</sub>” in the following sections and appears to contribute to the prolonged nature of the ADP and the refractory period.

What are the critical features of repetitive current pulses that upregulate I<sub>h</sub>? Here, we examined the possibility that the amplitude of the ADP may be influenced by the entry of Ca<sup>2+</sup> into thalamocortical neurons. To test this hypothesis, we compared the amplitude of the ADP that follows single, long-duration current pulses (1–15 s, 200–400 pA) that initiated only one rebound low-threshold Ca<sup>2+</sup> spike (Figure 2A) to the amplitude of the ADP generated in the same neurons in response to the injection of 5–25 repetitive hyperpolarizing current pulses that each initiated rebound Ca<sup>2+</sup> spikes (4 Hz, 200–400 pA, 120 ms; Figure 2B).

The amplitude of the ADP obtained with repetitive pulses, in which each pulse is followed by a Ca<sup>2+</sup> spike, was larger than that following a single, long-duration pulse of equal total injected charge but with only one

rebound Ca<sup>2+</sup> spike at the end of the pulse ( $n = 5$ – $10$  per point; Figure 2C). A semi-logarithmic plot of the data yielded a linear relation between the size of the ADP and the injected charge, yet the curve relating charge injected with repetitive pulses to the ADP displayed a larger slope than that corresponding to single pulses (Figure 2C [inset]). These results indicate that repetitive negative current pulses are more efficient in generating a slow ADP than single pulses. Therefore, induction of an ADP is facilitated if Ca<sup>2+</sup> entry through voltage-gated channels is evoked concomitantly with activation of I<sub>h</sub>. This conclusion is further supported by the effect of local application of Ni<sup>2+</sup> (2–5 mM in micropipette) on the amplitude of this event (Figures 3A–3D). Reduction of Ca<sup>2+</sup> spikes following application of Ni<sup>2+</sup> ions resulted in a substantial reduction of the size of the ADP (by  $56.0\% \pm 4.1\%$ ,  $n = 5$ ,  $p < 0.002$ ; Figures 3A, 3B, and 3D) without affecting the response of the neuron to a 120 ms duration hyperpolarizing current pulse that generates a depolarizing sag owing to activation of I<sub>h</sub> (Figure 3C). The residual rebound depolarizations following each current pulse in the presence of Ni<sup>2+</sup> were due to the activation of I<sub>h</sub>, since they were blocked by local

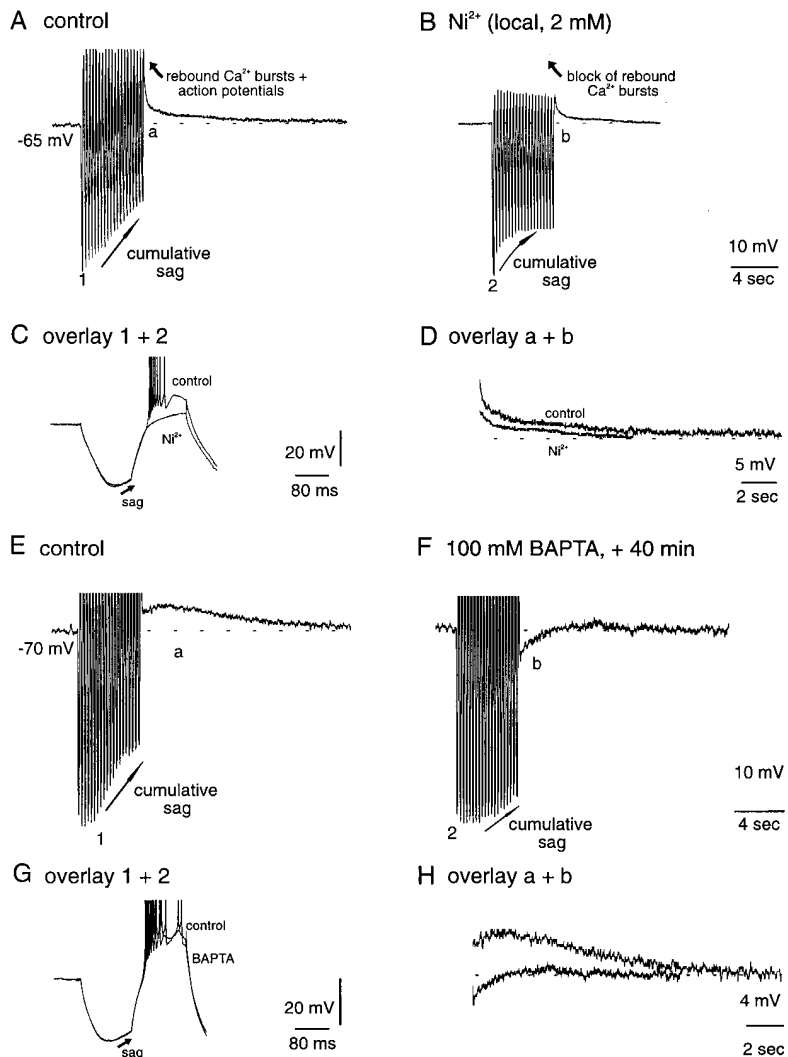


Figure 3. Interfering with  $\text{Ca}^{2+}$  Influx through Rebound  $\text{Ca}^{2+}$  Spikes Reduces the Amplitude of the Slow ADP

(A) ADP generated by a series of repetitive hyperpolarizing current injections (4 Hz,  $-500$  pA, 20 pulses, each 120 ms). During the pulses, the cell gradually depolarizes and displays an ADP following the end of the current injections.

(B) Local application of  $\text{Ni}^{2+}$  ions (2 mM in micropipette) abolishes the rebound  $\text{Ca}^{2+}$  bursts and reduces the ADP. Furthermore, the depolarization displayed during the repetitive current injections (cumulative sag) is reduced in extent and saturates after eight pulses.

(C) Overlay of the membrane potential response to the first of the 20 current injections at an expanded time scale under control conditions and in the presence of  $\text{Ni}^{2+}$  ions.

(D) Overlay of the ADP under control conditions and in the presence of  $\text{Ni}^{2+}$  ions.

(E) A series of repetitive hyperpolarizing current injections leads to a cumulative sag followed by an ADP after the pulses (4 Hz,  $-500$  pA, 20 pulses, each 120 ms).

(F) Following perfusion of this cell with BAPTA (100 mM in recording pipette), the ADP is abolished and an after-hyperpolarization remains.

(G) Overlay of the membrane potential response to the first of the 20 current injections at an expanded time scale under control conditions and following 40 min of perfusion with BAPTA.

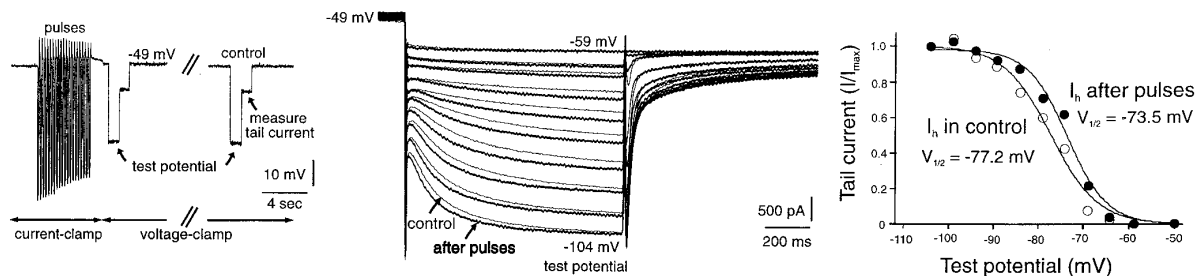
(H) Overlay of the ADP under control conditions and the membrane potential response following perfusion with BAPTA.

application of either  $\text{Cs}^+$  (20 mM in micropipette) or ZD7288 (1 mM; data not shown). In the presence of  $\text{Ni}^{2+}$ , the slow ADP generated by 20 repetitive hyperpolarizing pulses (4 Hz) was not significantly different from that generated in response to a single hyperpolarization of 5 s duration and equal current amplitude ( $n = 5$ ,  $p > 0.05$ ; data not shown). Reduced upregulation of  $I_h$  in the presence of  $\text{Ni}^{2+}$  was also observed by inspecting the envelope of peak hyperpolarizing potential reached during the repetitive current injections (Figures 3A and 3B; "cumulative sag"). This envelope characterizes the progressive activation of  $I_h$ , as it is abolished in the presence of extracellular  $\text{Cs}^+$  ( $n = 5$ ; Bal and McCormick, 1996). Whereas the time course of this cumulative sag was characterized by a nearly linear, nonsaturating depolarization under control conditions, in the presence of  $\text{Ni}^{2+}$  ions it turned into a weaker depolarization, saturating after a few pulses and resembling the membrane potential envelope observed with single hyperpolarizing pulses (cf. Figure 2), indicating that  $\text{Ni}^{2+}$  interfered with  $\text{Ca}^{2+}$ -mediated effects on  $I_h$  but not with voltage-dependent activation.

Furthermore, intracellular perfusion of cells with the

$\text{Ca}^{2+}$  chelator BAPTA (25–100 mM in pipette) led to a total abolishment of the ADP ( $n = 8$ ) and revealed an after-hyperpolarization following the current injections, most likely due to hyperpolarizing  $\text{K}^+$  conductances activated during the conditioning protocol (Figures 3E and 3F). The more pronounced effect of intracellular  $\text{Ca}^{2+}$  chelation with BAPTA in comparison with prevention of  $\text{Ca}^{2+}$  influx by divalent cations suggests that some minimal level of intracellular  $\text{Ca}^{2+}$  may be required for the expression of  $I_h$  and the slow voltage gating during the current injections (Schwindt et al., 1992). Indeed, perfusion of cells with BAPTA not only prevented the ADP but also strongly reduced the slow cumulative sag during the repetitive current injections (Figures 3E and 3F) without affecting cellular input resistance or the fast sag potential (Figure 3G). Similar results were also obtained when EGTA (100 mM in pipette) instead of BAPTA was used to chelate intracellular  $\text{Ca}^{2+}$  (data not shown;  $n = 2$ ). In contrast to the effect of  $\text{Ni}^{2+}$ , application of tetrodotoxin (TTX) (local, 1–10  $\mu\text{M}$  in micropipette) to prevent  $\text{Na}^+$  influx via voltage-gated  $\text{Na}^+$  channels had no effect on the amplitude of the ADP ( $100.8\% \pm 2.4\%$  of control,  $n = 11$ ,  $p > 0.05$ ). These data support the

### A Repetitive current injections



### B Single current injections

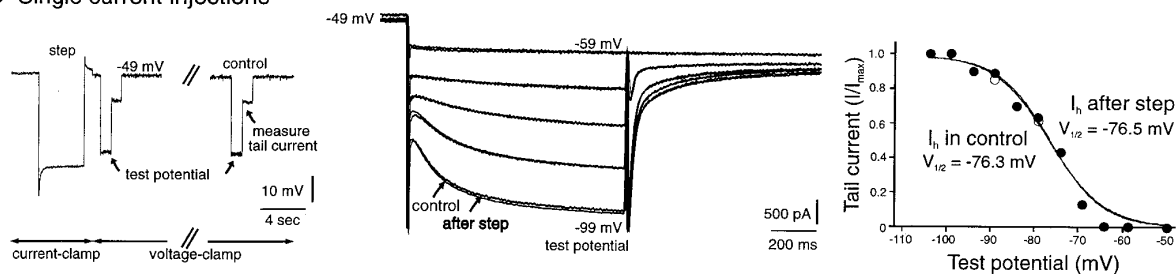


Figure 4. Repetitive Current Injections Induce a Shift in the Activation Curve of I<sub>h</sub>

(A) Repetitive negative current injections (4 Hz, 2 nA, 20 pulses, 120 ms) are applied to the cell from a membrane potential outside the activation range of I<sub>h</sub> (−49 mV). Cells are then voltage clamped and stepped to hyperpolarized voltages (test potential) for 1 s to activate I<sub>h</sub>. Before stepping back to the original holding potential, cells are held at −59 mV for 1 s to measure tail current amplitudes. The same protocol is repeated 10–15 s after the end of repetitive current injections. Only one test potential is tested following each set of hyperpolarizing current pulses. Overlay of I<sub>h</sub> responses 1 s after application of the conditioning train (after pulses) and 10–15 s later (control). The amplitude of the I<sub>h</sub> response under upregulated conditions (closed circles) is enhanced compared to control (open circles). Quantification of the tail current and fitting to a Boltzmann curve (see Experimental Procedures) reveals a positive shift in the activation curve of I<sub>h</sub> by 3.7 mV.

(B) Same experimental protocol as in (A), but repetitive current injections are replaced by a single, 5 s constant current injection of the same amplitude. No difference in I<sub>h</sub> responses is observed under test and control conditions. The activation curve of I<sub>h</sub> is not shifted to the right. All data are from the same cell.

idea that Ca<sup>2+</sup> entry during rebound Ca<sup>2+</sup> spikes enhances the slow ADP in thalamocortical cells.

To biophysically characterize possible effects of Ca<sup>2+</sup> on I<sub>h</sub>, the activation curve of this current was measured in the upregulated and in the control state (Figure 4). Cells were held at potentials well outside the activation range of I<sub>h</sub> by direct current injection (e.g., −45 to −52 mV), and repetitive negative current pulses (4 Hz, 20 pulses, 120 ms) sufficiently large to ensure generation of rebound Ca<sup>2+</sup> bursts at these depolarized potentials (1.5–2 nA) were applied while action potentials were blocked with local application of TTX (1–10 μM). Voltage-clamp was imposed 1 s after the last hyperpolarizing current pulse (Figure 4A), a time during which the ADP measured in current clamp was at its peak values (cf. Figures 2 and 3).

In voltage clamp, steps to increasing hyperpolarizing potentials were applied that covered the full activation range of I<sub>h</sub>, and the characteristics of the evoked I<sub>h</sub> responses were analyzed. Responses of I<sub>h</sub> obtained following repetitive current injections (i.e., under upregulated conditions) were significantly enhanced compared to the control responses obtained 10–15 s later (Figure 4A). This enhancement was most prominent in the middle of the activation range of I<sub>h</sub> and gradually decreased as voltage steps leading to maximal activation were applied. Plots of the activation curve of I<sub>h</sub>, based upon

the tail currents following activation of this current, revealed a half activation voltage  $V_{1/2} = -78.1 \pm 0.8$  mV under control conditions, in agreement with the values previously reported ( $n = 10$ ; Figure 4A; McCormick and Pape, 1990a). In contrast, during the period of the ADP induced by repetitive hyperpolarizing pulses, this activation curve was shifted to the right along the voltage axis by 1–4 mV (average half activation  $V_{1/2} = -75.8 \pm 0.8$  mV,  $n = 10$ ,  $p < 0.001$ ; Figure 4A). This shift in the activation curve most likely represents a lower limit, because at these depolarized potentials the recruitment of rebound Ca<sup>2+</sup> currents with short (120 ms) hyperpolarizing current pulses is diminished compared to around resting membrane potential due to voltage-dependent inactivation of this current (Huguenard, 1996). In contrast to the result with repetitive hyperpolarizing pulses, application of the same voltage-clamp protocol following a single hyperpolarizing step of 5 s duration and equal current injection amplitude did not reveal any changes in the activation curve, and the overlaid current responses under test and control conditions were indistinguishable (half activation  $V_{1/2} = -79.1 \pm 2.0$  mV versus  $-79.9 \pm 1.9$  mV control,  $n = 3$ ,  $p > 0.05$ ; Figure 4B). Thus, repetitive hyperpolarizations that both activate I<sub>h</sub> as well as generate rebound Ca<sup>2+</sup> spikes lead to an enhancement of I<sub>h</sub> through a positive shift of the activation curve of this current.

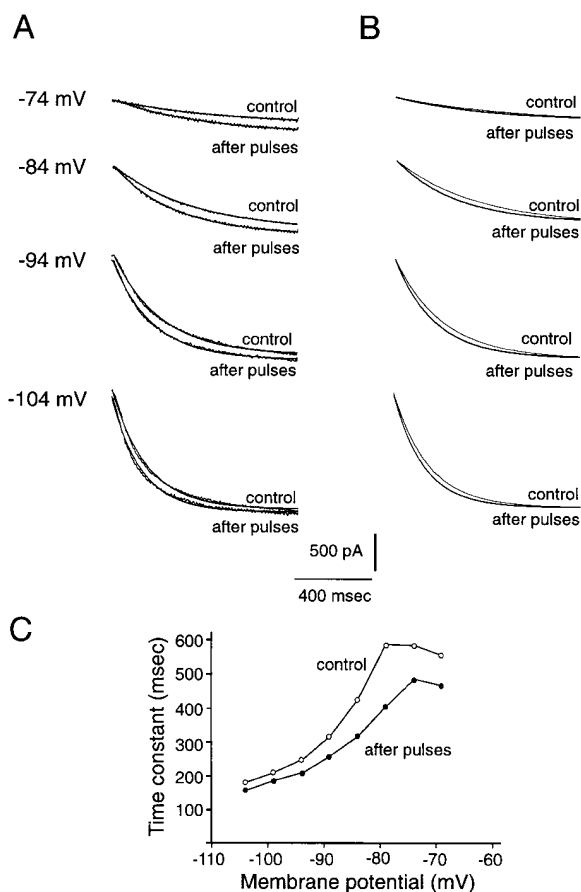


Figure 5. Enhancement of  $I_h$  with Repetitive Hyperpolarizations and Rebound  $Ca^{2+}$  Spikes Is Associated with an Acceleration in Activation Kinetics of This Current

(A) Comparison of the kinetics of  $I_h$  activation with and without preceding hyperpolarizing current pulses. These data are fit by single exponential functions.

(B) Comparison of the best fits of the data in (A) after compensation for changes in amplitude of  $I_h$ . Note the acceleration in activation kinetics following the repetitive hyperpolarizing pulses.

(C) Plot of the time constant for activation of  $I_h$  at different membrane potentials with and without preceding hyperpolarizing current pulses. These data were obtained from the cell in Figure 4.

Examination of the current responses characterizing  $I_h$  in the upregulated state and under control conditions revealed that the activation time course of  $I_h$  was accelerated ( $n = 10$ ; Figure 5A), and this acceleration was confirmed by monoexponential fits of the current traces (Figures 5B and 5C). The amplitude of the acceleration in kinetics was voltage dependent, being larger at more depolarized membrane potentials (Figure 5C).

If  $Ca^{2+}$  entry through T-channels during  $I_h$  activation is the trigger for upregulation of  $I_h$ , then experimental techniques to artificially (i.e., independently of  $Ca^{2+}$ -channels) manipulate the intracellular levels of  $Ca^{2+}$  should also enhance  $I_h$ . Flash photolysis of caged  $Ca^{2+}$  via a photolysable  $Ca^{2+}$  chelator (DM-Nitrophen, 70 mM in micropipette, 60%–75%  $Ca^{2+}$ -loaded; Kaplan, 1990; Zucker, 1993) was used to rapidly elevate  $Ca^{2+}$  in thalamocortical cells while simultaneously monitoring  $I_h$ . Microelectrodes, instead of patch pipettes, were used to

fill the cells with DM-Nitrophen in order to minimize the perturbation of endogenous  $Ca^{2+}$  buffers and second messenger systems. A brief flash of UV light (see Experimental Procedures), given following the intracellular recording of the cell for at least 45 min to allow the DM-Nitrophen ample time to diffuse throughout the cell, liberates  $Ca^{2+}$  from the chelator and is expected to increase  $[Ca^{2+}]_i$  into the micromolar range (Zucker, 1993). In current-clamp recordings, delivery of a flash while the cells were at potentials of  $-64$  to  $-82$  mV results in a 0.5–4 mV depolarization, after a 1–4 s delay ( $n = 27$ ; Figure 6A). This slow depolarization was associated with a decrease in the amplitude of the rebound low-threshold  $Ca^{2+}$  spikes, and consequently a decrease in the activation of  $Na^+$ -mediated action potentials, similar to the ADP observed during the refractory period of spindle waves ( $n = 27$ ; Figure 6A; Bal and McCormick, 1996).

In 13 cells, the electrode's input resistance following perfusion with DM-Nitrophen was low enough ( $<90$  M $\Omega$ ) to allow current responses in the single-electrode voltage-clamp mode to be obtained (see Lancaster and Zucker, 1994). The  $I_h$  responses evoked by application of hyperpolarizing voltage commands were directly enhanced in amplitude following application of a UV flash in 11 of 13 cells (Figure 6B). The average enhancement was  $114\% \pm 2\%$  of control ( $p < 0.001$ ), ranged from 5%–55%, could be evoked up to 14 times within a cell, and was without a significant change in the size of the initial "leak" component of the current evoked by the voltage command ( $101.9\% \pm 1\%$  of control,  $n = 25$  responses,  $p > 0.05$ ). Maximal responses were obtained in cells that displayed spontaneous  $\delta$ -oscillations (McCormick and Pape, 1990a) during the 45 min perfusion period (upregulation  $28\% \pm 8\%$ ,  $n = 3$ ,  $p < 0.02$ ), suggesting that cells with relatively low basal  $I_h$  are most responsive to increases in intracellular  $Ca^{2+}$ .

The enhancement of  $I_h$  lasted 10–20 s after the UV flash (Figure 6B) and was characterized by a gradual increase in the response during the first two voltage steps (within 10 s), followed by recovery of the  $I_h$  response to its original level, thus matching the overall time course of the flash-induced depolarization obtained in current-clamp recordings (Figure 6A). Following block of  $I_h$  with the local application of the specific blockers ZD7288 (1 mM) or  $Cs^+$  (20 mM in micropipette), application of a flash response neither induced a membrane depolarization in current clamp nor induced changes in current responses to hyperpolarizing voltage steps ( $n = 8$ ; Figure 6C). To exclude the possibility that reactive byproducts of photolysis could be responsible for the flash-evoked increase in  $I_h$ , cells were also loaded with DM-Nitrophen without addition of  $Ca^{2+}$ . Application of a UV flash to these cells resulted in no significant change in  $I_h$  ( $n = 5$ ,  $p > 0.05$ ; Figure 6D). Furthermore, flash photolysis experiments were performed in the presence of the pH buffer HEPES (100 mM) added to the pipette containing DM-Nitrophen and  $Ca^{2+}$ , and enhancements (10%–20%) of  $I_h$  were still obtained ( $n = 3$ ), indicating that changes in pH related to photolysis of DM-Nitrophen are not the primary cause for the flash-induced upregulation of  $I_h$ .

These data unambiguously demonstrate that abrupt elevations in intracellular  $Ca^{2+}$  increase  $I_h$  and strongly

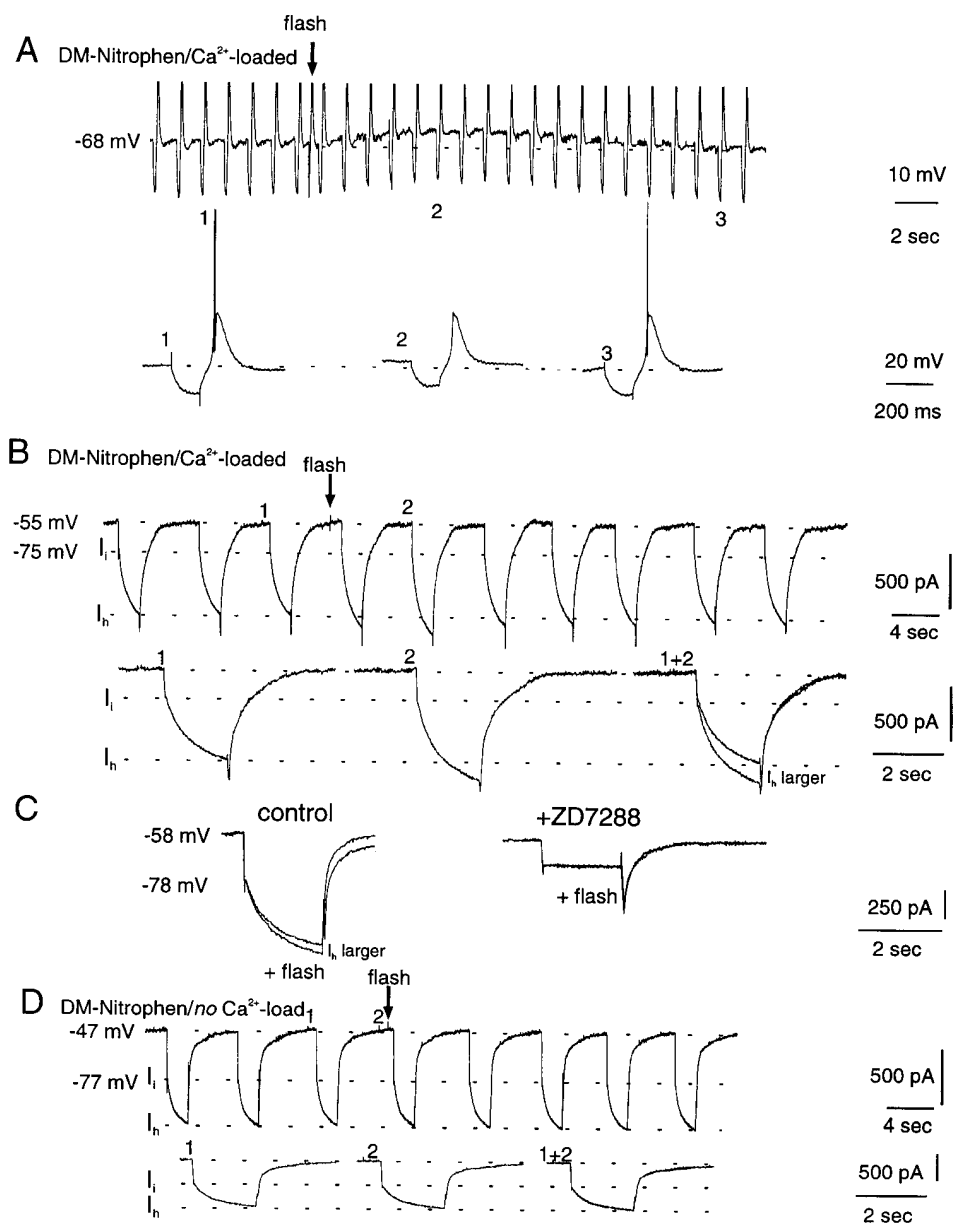


Figure 6. Flash Photolysis of Caged Ca<sup>2+</sup> Induces an Upregulation of I<sub>h</sub>

(A) Cell perfused with DM-Nitrophen (70 mM, 75% Ca<sup>2+</sup>-loaded) for ~50 min. Cell is injected with short (120 ms, -150 pA) hyperpolarizing current pulses to assess cellular responsiveness to hyperpolarizing inputs. Application of a flash (arrow) induces a slow depolarization associated with reduced amplitude of the rebound Ca<sup>2+</sup> spike in response to the injection of a constant current pulse. The peak amplitude of each rebound Ca<sup>2+</sup> spike is not shown. Expanded traces are depicted below (1, 2, and 3).

(B) In voltage clamp, delivery of a flash evokes an increase in I<sub>h</sub> without a major change in instantaneous current (I<sub>i</sub>). This cell was clamped at -55 mV and stepped repetitively to -75 mV. Expanded traces are presented below and overlaid for comparison (1 and 2).

(C) If I<sub>h</sub> is blocked by ZD7288 (local, 1 mM), flash photolysis of Ca<sup>2+</sup>-loaded DM-Nitrophen does not induce any changes in membrane current responses to hyperpolarizing voltages. Prior to application of ZD7288, application of a flash induced an increase in I<sub>h</sub> response (left). In the presence of ZD7288, I<sub>h</sub> was fully blocked and no further response was elicited (right).

(D) If cells are perfused with DM-Nitrophen that was not preloaded with Ca<sup>2+</sup>, application of a flash does not upregulate I<sub>h</sub>. The cell was recorded with an unloaded DM-Nitrophen-filled micropipette for 50 min. Then, voltage clamp was initiated and the cell stepped from -47 to -77 mV to elicit I<sub>h</sub> responses. Application of a flash (arrow) induced no change in either I<sub>h</sub> or the instantaneous current (I<sub>i</sub>). Selected responses are presented at an expanded time scale and overlaid for comparison. After offset of hyperpolarizing pulses, large, unclampable inward currents were usually observed that resulted from activation of low-threshold Ca<sup>2+</sup> currents (see [B] and [C]).

suggest that Ca<sup>2+</sup>, whether acting directly or indirectly, contributes to the upregulation of I<sub>h</sub> during the spindle-induced refractory period. However, in contrast to these results, no upregulation of I<sub>h</sub> was obtained when cells

were perfused via whole-cell patch pipettes containing a solution with highly buffered micromolar concentrations of free Ca<sup>2+</sup> (10 mM EGTA, pCa 5-6; data not shown) as recently reported (Budde et al., 1997).

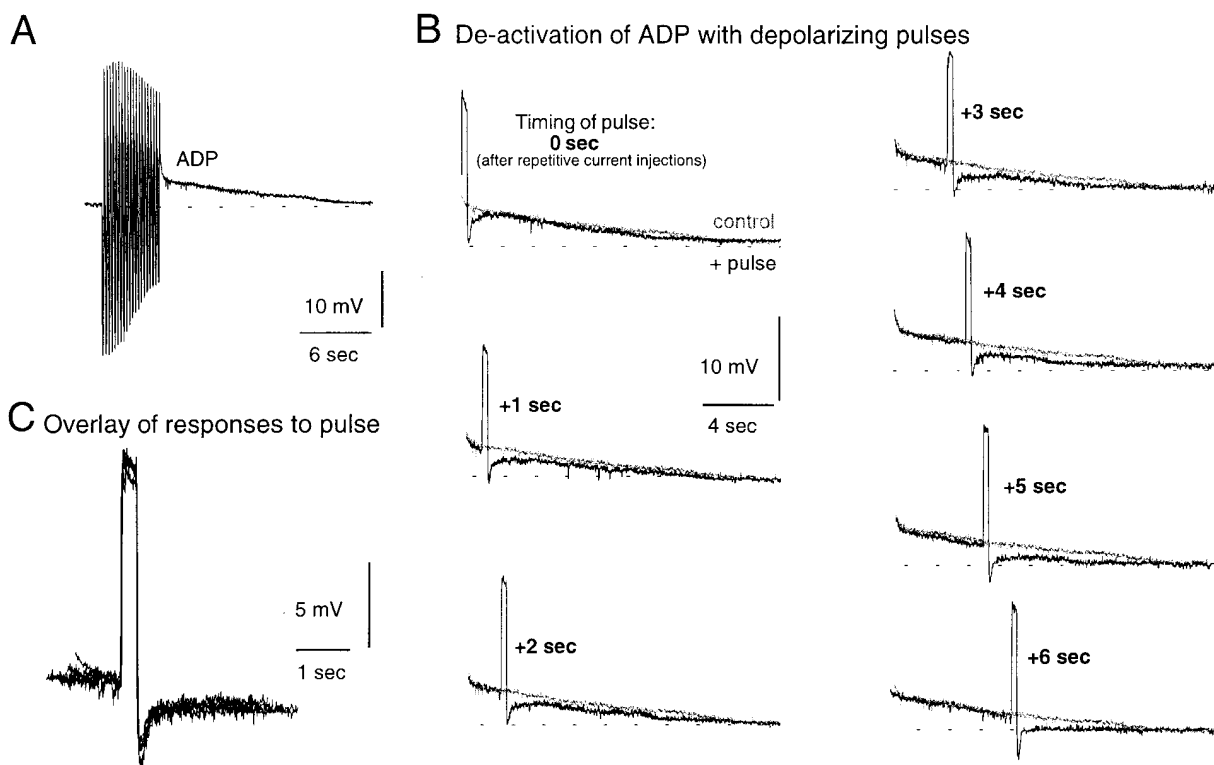


Figure 7. Deactivation of the ADP Depends upon the Timing of the Application of Depolarizing Pulses

(A) Application of a series of repetitive current injections (4 Hz,  $-500$  pA, 20 pulses, each 120 ms) induces a slowly decaying ADP. (B) Application of a short depolarizing current pulse (300 ms, 500 pA) to deactivate  $I_h$  at various times during the ADP (0, +1, +2, ..., +6 s). This pulse, applied during the early portions of the ADP (0–3 s), only weakly affects the ADP, whereas the same pulse applied later (4–6 s) strongly reduces the ADP. Control ADP (from [A]) is overlaid over each response in light gray. (C) Overlay of membrane potential responses to the depolarizing current injected at various times during the ADP.

The h-current is deactivated by depolarization (McCormick and Pape, 1990a), and we have previously demonstrated that a strong depolarization applied during the ADP may abolish it (Bal and McCormick, 1996). Here, we examined the time course of this depolarization-induced reduction of the ADP (Figure 7). Application of 0.5–1 nA, 120–300 ms duration depolarizing steps during the ADP (resulting in 12–25 mV of membrane depolarization,  $n = 6$ ) revealed that the ADP was differentially sensitive to such perturbative current injections, depending on their timing (Figures 7A and 7B). Thus, a depolarizing pulse injected immediately at the end of the repetitive current injections was without any effect on the remainder of the ADP, as evidenced by overlay of the control trace (no depolarization during the ADP) with the test response (Figure 7B; 0 s). Similarly, current injections up to 2–3 s following the last hyperpolarizing current pulse only weakly reduced the ADP. The same pulses applied later than 3 s lead to a substantial reduction (Figure 7B, 4 and 5 s traces) or a complete block (Figure 7B, 6 s trace) of the ADP. Similar findings were observed for all six cells investigated, with the critical time for ADP deactivation lying between 2 and 4 s. Overlay of the membrane responses to the depolarizing current injections revealed no significant change in their size, demonstrating that differences in input resistance did not account for the effect observed (Figure 7C).

These results indicate that there are both early and late time-dependent processes involved in the generation of the ADP.

#### Discussion

In the present study, we demonstrate how an interaction between the electrophysiological properties of the hyperpolarization-activated cation current  $I_h$  and the second messenger systems that regulate this current can generate a slow periodicity in synchronized thalamocortical oscillations. We propose that during a spindle or a bicuculline-induced paroxysmal oscillation (Steriade et al., 1993; von Krosigk et al., 1993), rebound  $Ca^{2+}$  spikes lead to an increase in  $[Ca^{2+}]_i$  that, in association with IPSPs due to synaptic activity of PGN cells, both voltage-gates and upregulates  $I_h$ . The ensuing membrane depolarization reduces the probability that IPSPs arriving from discharges of PGN neurons will result in rebound low-threshold  $Ca^{2+}$  spikes in thalamocortical neurons. This effect, occurring in a population of synchronously oscillating neurons, results in a gradual abolition of the network activity and the generation of the refractory period (see Bal and McCormick, 1996). During the refractory period,  $Ca^{2+}$  sequestration and slow decay of the upregulated  $I_h$  results in repolarization of the cells, thus rendering them responsive to IPSPs again.

### The Upregulation of I<sub>h</sub> by Ca<sup>2+</sup>

Our data provide direct evidence for an involvement of [Ca<sup>2+</sup>]<sub>i</sub> in the modulation of I<sub>h</sub> and the slow ADP in thalamocortical cells following repetitive hyperpolarization and rebound Ca<sup>2+</sup> spikes. Through the application of hybrid current-clamp/voltage-clamp techniques, we have demonstrated that the time period of the slow ADP is associated with a shift in the activation curve of I<sub>h</sub> to more positive levels (Figure 4), a marked slowing of the deactivation kinetics of I<sub>h</sub> (Figure 1), and an increase in the rate of activation of I<sub>h</sub> (Figure 5). Similarly, direct increases in [Ca<sup>2+</sup>]<sub>i</sub> with photolysis-mediated release of caged Ca<sup>2+</sup> also consistently revealed increases in the amplitude of I<sub>h</sub> (Figure 6). Additional evidence for an enhancing role of increases in [Ca<sup>2+</sup>]<sub>i</sub> on I<sub>h</sub> is provided by the increased efficiency of repetitive hyperpolarizations to activate I<sub>h</sub> in comparison to equivalent single hyperpolarizations that do not result in repetitive rebound Ca<sup>2+</sup> spikes (Figure 2) and the depression of ADP amplitude following the application of the Ca<sup>2+</sup> channel blocker Ni<sup>2+</sup> or the intracellular injection of the Ca<sup>2+</sup> chelating agents BAPTA or EGTA (Figure 3).

These data help to resolve a long-standing debate over whether or not hyperpolarization-activated cation currents are sensitive to changes in [Ca<sup>2+</sup>]<sub>i</sub> (Hagiwara and Irisawa, 1989; Zaza et al., 1991; Pape, 1996; Budde et al., 1997). In experiments performed by Hagiwara and Irisawa, heart cells were perfused with solutions containing micromolar concentrations of free Ca<sup>2+</sup> via a whole-cell patch pipette, which induced a shift of the activation curve of the cardiac hyperpolarization-activated cation current (I<sub>h</sub>) to more positive membrane potentials. Based on biochemical experiments, the authors proposed a direct modulatory action of Ca<sup>2+</sup> onto f-channels. This conclusion, however, has not been verified in inside-out patches containing f-channels, where the free Ca<sup>2+</sup> concentration on the membrane facing the cytosol can be systematically buffered to the μM range (Zaza et al., 1991). Furthermore, recent studies of I<sub>h</sub> in thalamocortical cells or in primary afferent neurons maintained in slices *in vitro* have failed to demonstrate a shift in the activation curve of I<sub>h</sub> when free [Ca<sup>2+</sup>]<sub>i</sub> was varied in the whole-cell recording pipette (Ingram and Williams, 1996; Budde et al., 1997), a finding that we have also obtained. On the other hand, recordings in neocortical neurons with microelectrodes containing high concentrations of the Ca<sup>2+</sup> chelating agent BAPTA suggest that a minimal basal level of [Ca<sup>2+</sup>]<sub>i</sub> may be required for functional expression of hyperpolarization-activated cation currents (Schwindt et al., 1992; see also Figure 3).

Three questions that may be critical to understanding this apparently contradictory evidence remain unanswered. First, is the experimental verification of a Ca<sup>2+</sup>-mediated alteration of hyperpolarization-activated cation currents dependent on a cellular environment unperturbed by the electrophysiological recording technique used? Second, is the time course and spatial extent of increases in [Ca<sup>2+</sup>]<sub>i</sub> important in the enhancement of I<sub>h</sub>? Finally, is the enhancement of I<sub>h</sub> by Ca<sup>2+</sup> mediated indirectly through the modulation of a second messenger or dependent upon the coactivation of one?

Activation of low-threshold Ca<sup>2+</sup> spikes results in increases in [Ca<sup>2+</sup>]<sub>i</sub> throughout the soma and proximal

dendrites, rising to a peak in about 30 ms and slowly decaying over a period of seconds (at 22°C–25°C) (Zhou et al., 1997). Owing to this slow decay, repetitive activation of low-threshold Ca<sup>2+</sup> spikes at 2 Hz results in temporal summation of these Ca<sup>2+</sup> transients and a subsequent slow decay of [Ca<sup>2+</sup>]<sub>i</sub> over a period of ~10 s at room temperature (Munsch et al., 1997). Thus, activation of T-currents during repetitive hyperpolarizing current injections most likely leads to significant increases in intracellular Ca<sup>2+</sup> in at least the soma and proximal dendrites of thalamocortical cells and represents the major triggering event for the Ca<sup>2+</sup>-mediated upregulation of I<sub>h</sub>, although we cannot exclude that additional Ca<sup>2+</sup> release from internal stores (see Munsch et al., 1997) or entry of Ca<sup>2+</sup> through high voltage-activated channels may also contribute.

### The Mechanism of Action of Ca<sup>2+</sup>

Several observations in our data suggest that Ca<sup>2+</sup> may not directly modulate h-channels but rather may act through the generation of one or more second messenger compounds. First, the shift of the activation curve of I<sub>h</sub> induced following application of repetitive hyperpolarizations displays striking similarities to that induced following increases in cyclic nucleotide levels (e.g., cAMP, cGMP) induced by neurotransmitters (McCormick and Pape, 1990b; Pape and Mager, 1992). Thus, the enhancement was associated with a shift in the activation curve of this current and the maximal responses were not altered in size. Although it is possible that small changes in maximal conductance occurred (e.g., Hagiwara and Irisawa, 1989) that went undetected with our experimental techniques, our findings support the notion that it is primarily a shift in the voltage sensitivity of I<sub>h</sub> toward more depolarized potentials that contributes to enhanced activation of this current. Second, the time course of upregulation of I<sub>h</sub> induced by flash photolysis of caged Ca<sup>2+</sup> was characterized by a slow and gradual (over seconds) increase to its peak amplitude (Figure 6), which is temporarily incongruent with the fast concentration spike in Ca<sup>2+</sup> following photolysis of DM-nitrophen (Zucker, 1993). Previous investigations have demonstrated that the photolysis-mediated release of caged Ca<sup>2+</sup> leads to the activation of Ca<sup>2+</sup>-sensitive K<sup>+</sup> currents in hippocampal pyramidal cells with a latency to peak on the order of tens of milliseconds (Lancaster and Zucker, 1994). The slow time course of the flash-mediated upregulation of I<sub>h</sub> therefore suggests that the effects of Ca<sup>2+</sup> are mediated indirectly. Interestingly, several adenylyl cyclases (types I, III, and VIII) are stimulated by increases in [Ca<sup>2+</sup>]<sub>i</sub> in a manner that requires the presence of calmodulin (Cooper et al., 1994, 1995). *In situ* hybridization studies indicate that the message for type I and VIII adenylyl cyclases is expressed at significant levels in the thalamus, hippocampus, cortex, and cerebellum and at lower levels in brainstem and midbrain structures in the rat (Matsuoka et al., 1997; reviewed by Cooper et al., 1994). Thus, these enzymes could represent a substrate by which the Ca<sup>2+</sup>-mediated upregulation of I<sub>h</sub> is established.

Hyperpolarization-activated cation channels are structurally related to the cyclic nucleotide-gated channels

that are involved in a variety of cell functions (reviewed by Finn et al., 1996). The molecular basis for the modulation of these channels by cyclic nucleotides is biophysically characterized (Zagotta and Siegelbaum, 1996; Finn et al., 1996; Tibbs et al., 1997). Furthermore,  $\text{Ca}^{2+}$ /calmodulin has been reported to alter the affinity of these channels for cyclic nucleotides (Liu et al., 1994). Thus, in the case of  $I_h$ ,  $\text{Ca}^{2+}$  might in addition act to alter the affinity of h-channels for cyclic nucleotides. In preliminary experiments, we have found that at least part of the upregulation of  $I_h$  by repetitive hyperpolarizing pulses or photolysis of caged  $\text{Ca}^{2+}$  can be blocked by application of adenylyl cyclase inhibitors (Lüthi and McCormick, 1997, Soc. Neurosci., abstract).

Each refractory period reflects a multicomponent decay of several components, including raised intracellular  $\text{Ca}^{2+}$  levels, possible alterations in second messenger substances, and open ion channels in the cellular membrane. This complex dynamic interaction was studied by interfering with activation of  $I_h$  during the ADP by transiently forcing part of the underlying channels into a closed state (Figure 7). These experiments reveal that there are at least two time-dependent components of the ADP. During the first few seconds of the ADP, there appears to be a signal that allows  $I_h$  to become re-upregulated following deactivation with the depolarizing pulse. The finding that delivery of a depolarizing pulse may abolish the ADP during this later period suggests that the second messengers responsible for the upregulation of  $I_h$  have dissipated to such an extent that the remaining upregulated  $I_h$  did not result in a detectable ADP. Therefore, these data suggest that the prolonged decay of the ADP is at least in part due to h-channels whose persistence in the open configuration outlasts the availability of upregulatory compounds (e.g., Zufall et al., 1993; Tibbs et al., 1997).

In animals and humans, both normal synchronized thalamocortical rhythms such as spindle waves and abnormal rhythms such as spike-and-wave or absence seizures can exhibit slow periodicities on the order of seconds or tens of seconds (Terzano et al., 1985; Niedermeyer, 1990; Jandó et al., 1995; Contreras et al., 1997). We suggest that the  $\text{Ca}^{2+}$ -dependent upregulation of hyperpolarization-activated cation currents may be one of the major mechanisms by which these events spontaneously cease and therefore may form a novel avenue for the pharmacological control of these. This hypothesis remains to be explored.

#### Experimental Procedures

Male or female ferrets, ~2 months old, were deeply anesthetized with sodium pentobarbital (30 mg/kg intraperitoneally) and sacrificed by decapitation in accordance with Yale University Medical School guidelines for the use of animals in research. Sagittal slices (350–400  $\mu\text{m}$  thick) were prepared on a vibratome (Ted Pella) and maintained in an interface chamber (Fine Sciences Tools) at 34°C–35°C. The perfusion medium contained the following (in mM): 126 NaCl, 2.5 KCl, 1.2  $\text{MgSO}_4$ , 1.25  $\text{NaH}_2\text{PO}_4$ , 2  $\text{CaCl}_2$ , 26  $\text{NaHCO}_3$ , and 10 dextrose. Solutions were aerated with 95%  $\text{O}_2$ /5%  $\text{CO}_2$  to pH 7.4. Drugs were applied locally with the pressure-pulse technique in which small (1–10  $\mu\text{l}$ ) drops of drug solution were extruded from a broken micropipette (3–5  $\mu\text{m}$  tip diameter). Intracellular recording electrodes contained 2 M potassium acetate (sometimes 100 mM HEPES in addition) adjusted to pH 7.2–7.3. Intracellular recordings

were performed with micropipettes formed on a Sutter Instruments P-80/PC micropipette puller from medium-walled glass (IB100F, World Precision Instruments) and beveled on a Sutter Instruments beveler. Electrode resistances ranged between 80–120 M $\Omega$  for current-clamp recording and 50–90 M $\Omega$  for voltage-clamp recordings. Voltage clamp was performed using the discontinuous single-electrode voltage-clamp technique by an Axoclamp-2A amplifier (Axon Instruments) in which the output of the headstage was continuously monitored in order to ensure adequate settling time prior to the injection of current. Only those cells that exhibited stable resting membrane potentials of between –62 and –70 mV and input resistances in excess of 50 M $\Omega$  were included for analysis. Data were collected through a multi-channel encoding device (Neurodata Instruments) onto videotape for offline analysis. Data were analyzed with the use of an IBM 486 computer equipped with pClamp software. Statistical analysis was done using Student's *t* test. The time course of  $I_h$  in Figure 1 was fit according to the following equation:  $I_t = A_0 + A_1e^{-t/\tau_1} + A_2e^{-t/\tau_2}$ , where  $I_t$  is the amplitude of the current at time *t*;  $A_0$ ,  $A_1$ , and  $A_2$  are constants; and  $\tau_1$  and  $\tau_2$  are two time constants. For the  $I_h$  responses lasting 1 s in Figure 5, monoexponential fitting was used. The activation curves for  $I_h$  were fit according to the Boltzman equation:  $I/I_{\text{max}} = (1 + \exp[(V_m - V_{1/2})/s])^{-1}$ , where  $V_m$  is the membrane potential,  $V_{1/2}$  is the membrane potential at which  $G_h$  is half activated, *I* is the amplitude of the tail current, and *s* is the slope factor.

Flash photolysis of caged  $\text{Ca}^{2+}$  was used as an additional, independent approach to study the  $\text{Ca}^{2+}$  dependence of  $I_h$ . In intracellular recordings, the photolabile  $\text{Ca}^{2+}$  buffer DM-Nitrophen (70–100 mM, 60%–75%  $\text{Ca}^{2+}$ -loaded) was added to the intracellular sharp electrode solution. Impaled cells were perfused for at least 45 min with this solution, via 1 Hz application of –500 pA current injections for the entire period. Only cells that exhibited stable membrane potentials during the 1 to 2 hr of recording and in which the resistance of the microelectrode did not significantly increase (i.e., did not "block") were included for analysis. Photolysis of DM-Nitrophen was achieved through a Xenon Arc lamp (Rapp Flashlamp JML-C1 from HiTech Scientific, UK) that delivered a 1 ms UV flash following discharge of a capacitance (3470  $\mu\text{F}$ , 380 V). The UV flash covered most of the geniculate slice, although the most intense UV energy was focused on the region of the recorded neuron. ZD7288 was obtained from Tocris Cookson (UK) and DM-nitrophen was obtained from Calbiochem. All other drugs were obtained from Sigma.

#### Acknowledgments

We thank Fred Sigworth, Thierry Bal, and Mavi Sanchez-Vives for stimulating discussions in the course of this study. A. L. was supported by a fellowship from the Swiss National Science Foundation, and D. A. M. was supported by the National Institutes of Health, the McKnight Foundation, and the Human Frontier Scientific Program.

Received December 23, 1997; revised January 16, 1998.

#### References

- Andersen, P., and Andersson, S.A. (1968). *Physiological Basis of the Alpha Rhythm* (New York: Appleton-Century-Crofts).
- Bal, T., and McCormick, D.A. (1996). What stops synchronized thalamocortical oscillations? *Neuron* 17, 297–308.
- Bal, T., von Krosigk, M., and McCormick, D.A. (1995a). Synaptic and membrane mechanisms underlying synchronized oscillations in the ferret lateral geniculate nucleus in vitro. *J. Physiol.* 483, 641–663.
- Bal, T., von Krosigk, M., and McCormick, D.A. (1995b). Role of the ferret perigeniculate nucleus in the generation of synchronized oscillations in vitro. *J. Physiol.* 483, 665–685.
- BoSmith, R.E., Briggs, I., and Sturgess, N.C. (1993). Inhibitory actions of ZENECA ZD7288 on whole-cell hyperpolarization activated inward current ( $I_h$ ) in guinea-pig dissociated sinoatrial node cells. *Br. J. Pharmacol.* 110, 343–349.
- Budde, T., Biella, G., Munsch, T., and Pape, H.-C. (1997). Lack of regulation by intracellular  $\text{Ca}^{2+}$  of the hyperpolarization-activated cation current in rat thalamic neurones. *J. Physiol.* 503, 79–85.

- Contreras, D., Destexhe, A., Sejnowski, T.J., and Steriade, M. (1997). Spatiotemporal patterns of spindle oscillations in cortex and thalamus. *J. Neurosci.* *17*, 1179–1196.
- Cooper, D.M.F., Mons, N., and Fagan, K. (1994). Ca<sup>2+</sup>-sensitive adenylyl cyclases. *Cell. Signaling* *6*, 823–840.
- Cooper, D.M.F., Mons, N., and Karpen, J.W. (1995). Adenylyl cyclases and the interaction between calcium and cAMP signalling. *Nature* *374*, 421–424.
- Destexhe, A., Bal, T., McCormick, D.A., and Sejnowski, T.J. (1996). Ionic mechanisms underlying synchronized oscillations and propagating waves in a model of ferret thalamic slices. *J. Neurophysiol.* *76*, 2049–2070.
- Finn, J.T., Grunwald, M.E., and Yau, K.-W. (1996). Cyclic nucleotide-gated ion channels: an extended family with diverse functions. *Annu. Rev. Physiol.* *58*, 395–426.
- Hagiwara, N., and Irisawa, H. (1989). Modulation by intracellular Ca<sup>2+</sup> of the hyperpolarization-activated inward current in rabbit single sino-atrial node cells. *J. Physiol.* *409*, 121–141.
- Harris, N.C., and Constanti, A. (1995). Mechanism of block by ZD 7288 of the hyperpolarization-activated inward rectifying current in guinea pig substantia nigra neurons in vitro. *J. Neurophysiol.* *74*, 2366–2378.
- Huguenard, J.R. (1996). Low-threshold calcium currents in central nervous system neurons. *Annu. Rev. Physiol.* *58*, 329–348.
- Huguenard, J.R., and McCormick, D.A. (1992). Simulation of the currents involved in rhythmic oscillations in thalamic relay neurons. *J. Neurophysiol.* *68*, 1373–1383.
- Ingram, S.L., and Williams, J.T. (1996). Modulation of the hyperpolarization-activated current (I<sub>h</sub>) by cyclic nucleotides in guinea-pig primary afferent neurons. *J. Physiol.* *492*, 97–106.
- Jandó, G., Carpi, D., Kandel, A., Urioste, R., Horvath, Z., Pierre, E., Vadi, D., Vadasz, C., Buzsáki, G. (1995). Spike-and-wave epilepsy in rats: sex differences and inheritance of physiological traits. *Neuroscience* *64*, 301–317.
- Jones, E.G. (1985). *The Thalamus* (New York: Plenum).
- Kaplan, J.H. (1990). Photochemical manipulation of divalent cation levels. *Annu. Rev. Physiol.* *52*, 897–914.
- Kim, U., Bal, T., and McCormick, D.A. (1995). Spindle waves are propagating synchronized oscillations in the ferret LGNd in vitro. *J. Neurophysiol.* *74*, 1301–1323.
- Lancaster, B., and Zucker, R.S. (1994). Photolytic manipulation of Ca<sup>2+</sup> and the time course of slow, Ca<sup>2+</sup>-activated K<sup>+</sup> current in rat hippocampal neurones. *J. Physiol.* *475*, 229–239.
- Lee, K.H., and McCormick, D.A. (1996). Abolition of spindle oscillations by serotonin and norepinephrine in the ferret lateral geniculate and perigeniculate nuclei in vitro. *Neuron* *17*, 309–321.
- Leresche, N., Lightowler, S., Soltesz, I., Jassik-Gerschenfeld, D., and Crunelli, V. (1991). Low-frequency oscillatory activities intrinsic to rat and cat thalamocortical cells. *J. Physiol.* *441*, 155–174.
- Liu, M., Chen, T.-Y., Ahamed, B., Li, J., and Yau, K.-W. (1994). Calcium-calmodulin modulation of the olfactory cyclic nucleotide-gated cation channel. *Science* *266*, 1348–1354.
- Matsuoka, I., Suzuki, Y., Defer, N., Nakanishi, H., and Hanoune, J. (1997). Differential expression of type I, II, and V adenylyl cyclase genes in the postnatal developing rat brain. *J. Neurochem.* *68*, 498–506.
- McCormick, D.A., and Pape, H.-C. (1990a). Properties of a hyperpolarization-activated cation current and its role in rhythmic oscillation in thalamic relay neurones. *J. Physiol.* *431*, 291–318.
- McCormick, D.A., and Pape, H.-C. (1990b). Noradrenergic and serotonergic modulation of a hyperpolarization-activated cation current in thalamic relay neurones. *J. Physiol.* *431*, 319–342.
- McCormick, D.A., and Huguenard, J.R. (1992). A model of the electrophysiological properties of thalamocortical relay neurons. *J. Neurophysiol.* *68*, 1384–1400.
- McCormick, D.A., and Bal, T. (1997). Sleep and arousal: thalamocortical mechanisms. *Annu. Rev. Neurosci.* *20*, 185–215.
- Munsch, T., Budde, T., and Pape, H.-C. (1997). Voltage-activated intracellular calcium transients in thalamic relay cells and interneurons. *Neuroreport* *8*, 2411–2418.
- Niedermeyer, E. (1990). *The Epilepsies: Diagnosis and Management* (Baltimore, MD: Urban and Schwarzenberg).
- Pape, H.-C. (1996). Queer current and pacemaker: the hyperpolarization-activated cation current in neurons. *Annu. Rev. Physiol.* *58*, 299–327.
- Pape, H.-C., and Mager, R. (1992). Nitric oxide controls oscillatory activity in thalamocortical neurons. *Neuron* *9*, 441–448.
- Schwindt, P.C., Spain, W.J., and Crill, W.E. (1992). Effects of intracellular calcium chelation on voltage-dependent and calcium-dependent currents in cat neocortical neurons. *Neuroscience* *47*, 571–578.
- Soltesz, I., Lightowler, S., Leresche, N., Jassik-Gerschenfeld, D., Pollard, C.E., and Crunelli, V. (1991). Two inward currents and the transformation of low-frequency oscillations of rat and cat thalamocortical cells. *J. Physiol.* *441*, 175–197.
- Steriade, M., and Deschênes, M. (1984). The thalamus as a neuronal oscillator. *Brain Res. Rev.* *8*, 1–63.
- Steriade, M., McCormick, D.A., and Sejnowski, T.J. (1993). Thalamocortical oscillations in the sleeping and aroused brain. *Science* *262*, 679–685.
- Steriade, M., Jones, E.G., and McCormick, D.A. (1997). *Thalamus. Vol. 1: Organisation and Function*. (New York: Elsevier Science).
- Terzano, M.G., Mancina, D., Salati, M.R., Costani, G., Decembrino, A., and Parrino, L. (1985). The cyclic alternating pattern as a physiologic component of normal NREM sleep. *Sleep* *8*, 137–145.
- Tibbs, G.R., Goulding, E.H., and Siegelbaum, S.A. (1997). Allosteric activation and tuning of ligand efficacy in cyclic nucleotide-gated channels. *Nature* *386*, 612–615.
- von Krosigk, M., Bal, T., and McCormick, D.A. (1993). Cellular mechanisms of a synchronized oscillation in the thalamus. *Science* *261*, 361–364.
- Williams, S.R., Turner, J.P., Hughes, S.W., and Crunelli, V. (1997). On the nature of anomalous rectification in thalamocortical neurones of the cat ventrobasal thalamus in vitro. *J. Physiol.* *505*, 727–747.
- Zagotta, W.N., and Siegelbaum, S.A. (1996). Structure and function of cyclic nucleotide-gated channels. *Annu. Rev. Neurosci.* *19*, 235–263.
- Zaza, A., Maccaferri, G., Mangoni, M., and DiFrancesco, D. (1991). Intracellular calcium does not directly modulate cardiac pacemaker (i) channels. *Pflügers Arch.* *419*, 662–664.
- Zhou, Q., Godwin, D.W., O'Malley, D.M., and Adams, P.R. (1997). Visualization of calcium influx through channels that shape the burst and tonic firing modes of thalamic relay cells. *J. Neurophysiol.* *77*, 2816–2825.
- Zucker, R.S. (1993). The calcium concentration clamp: spikes and reversible pulses using the photolabile chelator DM-nitrophen. *Cell Calcium* *14*, 87–100.
- Zufall, F., Hatt, H., and Firestein, S. (1993). Rapid application and removal of second messengers to cyclic nucleotide-gated channels from olfactory epithelium. *Proc. Natl. Acad. Sci. USA* *90*, 9335–9339.